British Journal of Pharmacology

DOI:10.1111/j.1476-5381.2011.01783.x
www.brjpharmacol.org

RESEARCH PAPER

The neuroregenerative mechanism mediated by the Hsp90-binding immunophilin FKBP52 resembles the early steps of neuronal differentiation

HR Quintá and MD Galigniana

Instituto de Biología y Medicina Experimental-CONICET and Departamento de Química Biológica, Facultad de Ciencias Exactas y Naturales, Universidad de Buenos Aires, Buenos Aires, Argentina

Correspondence
Dr Mario D. Galigniana, Instituto de Biología y Medicina Experimental (IBYME), Vuelta de Obligado 2490, Buenos Aires (C1428ADN), Argentina. E-mail: mgaligniana@conicet.gov.ar; mgali@qb.fcen.uba.ar

Keywords
tacrolimus; immunophilins; TPR proteins; FKBP52; Hsp90; p23; synapsin; tau; neuronal differentiation; neuroregeneration; astrocytes

Received
11 May 2011
Revised
28 September 2011
Accepted
3 November 2011

BACKGROUND AND PURPOSE
The immunosuppressive macrolide FK506 (tacrolimus) shows neuroregenerative action by a mechanism that appears to involve the Hsp90-binding immunophilin FKBP52. This study analyses some aspects of the early steps of neuronal differentiation and neuroregeneration.

EXPERIMENTAL APPROACH
Undifferentiated murine neuroblastoma cells and hippocampal neurones isolated from embryonic day-17 rat embryos were induced to differentiate with FK506. Subcellular relocalization of FKBP52, Hsp90 and its co-chaperone p23 was analysed by indirect immunofluorescence confocal microscopy and by Western blots of axonal fractions isolated from cells grown on a porous transwell cell culture chamber. Neuroregeneration was evaluated using a scratch-wound assay.

KEY RESULTS
In undifferentiated cells, FKBP52, Hsp90 and p23 are located in the cell nucleus, forming an annular structure that disassembles when the differentiation process is triggered by FK506. This was observed in the N2a cell line and in hippocampal neurones. More importantly, the annular structure of chaperones is reassembled after damaging the neurones, whereas FK506 prompts their rapid regeneration, a process linked to the subcellular redistribution of the heterocomplex.

CONCLUSIONS AND IMPLICATIONS
There is a direct relationship between the disassembly of the chaperone complex and the progression of neuronal differentiation upon stimulation with the immunophilin ligand FK506. Both neuronal differentiation and neuroregeneration appear to be mechanistically linked, so the elucidation of one mechanism may lead to unravel the properties of the other. This study also implies that the discovery of FK506 derivatives, devoid of immunosuppressive action, would be therapeutically significant for neurotrophic use.

Abbreviations
DIV, days *in vitro*; E17 cells, hippocampal neurones isolated from embryonic day-17 rat embryos; FKBP, FK506-binding protein; GFAP, glial fibrillary acidic protein; GR, glucocorticoid receptor; Hsp, heat-shock protein; N2a, neuroblastoma cell line; PPIase, peptidyl-prolyl-(*cis*/*trans*) isomerase; TPR, tetratricopeptide repeats

Introduction

FK506 (tacrolimus) is a natural macrolide first isolated from the bacterium *Streptomyces tsukubaensis* (Kino *et al.*, 1987). FK506 shows profound immunosuppressive activities both *in vitro* and *in vivo*, and is effective in a wide variety of models of experimental transplantation and autoimmunity. In addition to its obvious clinical importance, the discovery of FK506 yielded new insights into the mechanisms underlying the activation of T-cells and its use is likely to impart even more important scientific information. From 1989, it has been used for the prevention of liver transplant rejection since 1989 and its use has subsequently been extended to the transplantation of other organs (Kapturczak *et al.*, 2004; Vicari-Christensen *et al.*, 2009; Wallemacq *et al.*, 2009). The immunosuppressant effect of FK506 depends on its binding to the low molecular weight immunophilin, FK506 binding protein (FKBP)12, and the FK506•FKBP12 complex is a selective inhibitory factor for the PP2B/calcineurin activity of T-cells (Liu *et al.*, 1992). More interestingly, FK506 also exhibits neuroprotective and neurotrophic effects (Gold and Villafranca, 2003), although the mechanism for this activity is totally unknown. The neurotrophic action was not abolished by knockout of FKBP12, which implies that other FK506-binding proteins should be involved. It was first suggested that FKBP52 could be a key factor as antibodies against this high molecular weight immunophilin prevented the neurotrophic action of FK506 (Gold *et al.*, 1999). In a recent study, the key role of FKBP52 in neuronal differentiation was confirmed by silencing its expression and it was also proposed that the balance between FKBP52 and its closely-related partner FKBP51 is important for the efficient progression of differentiation (Quintá *et al.*, 2010).

FKBP52 is a 52 kDa protein with chaperone properties (Davies and Sanchez, 2005) and is a target of FK506. The drug binds to the peptidyl-prolyl-(*cis*/*trans*) isomerase (PPIase) domain of the protein, which is the characteristic domain of the entire immunophilin family. The PPIase domain of FKBP52 shares 55% homology with the smaller but better-studied immunophilin, FKBP12 (Callebaut *et al.*, 1992). Unlike FKBP12, however, FKBP52 does not mediate the immunosuppressive actions of FK506. In addition to the PPIase domain, FKBP52 also has a series of tetratricopeptide repeat (TPR) domains, which serve as the binding site for the ubiquitous and abundant molecular heat-shock protein of 90 kDa, Hsp90. It is this property as a TPR protein that best characterizes the known cellular roles of FKBP52 (Sivils *et al.*, 2011). Since its discovery, most of the known biological properties of FKBP52 have always been related to its association with Hsp90, particularly as a key component of the steroid-receptor heterocomplex. Nonetheless, its biological role in the cell as an independent factor not associated with receptors is still poorly understood.

We have recently reported that there is a strong induction of FKBP52 expression during the early steps of the FK506-dependent differentiation of neuronal cells (Quintá *et al.*, 2010). Both Hsp90 and the Hsp90-associated co-chaperone p23 are also strongly induced. Even though all three proteins, FKBP52, Hsp90 and p23, are known to form heterocomplexes that bind the glucocorticoid receptor (GR) (Echeverria *et al.*, 2009; Galigniana *et al.*, 2010a), the effect of FK506 on neuronal differentiation was shown to be independent of the expression of GR. More interestingly, the FKBP52•Hsp90•p23 complex is primarily nuclear in undifferentiated cells and is located along the nuclear lamina. More interestingly, upon stimulation of the cells with FK506, the heterocomplex redistributes to the cytoplasm. It is unclear whether or not the existence of this nuclear structure and the disassembly of the chaperones are required to initiate the differentiation programme. In this study, we have evaluated the subcellular rearrangement of the FKBP52-based heterocomplex in cells stimulated with FK506 without the addition of any other trophic factor, so the effects could be solely assigned to the drug. This study also looked for any parallelism between the events triggered during the neurodifferentiation process in a cell line model and in primary cultures of embryonic hippocampal cells, with the events that take place during neuronal regeneration after the mechanical damage of the neurites.

Methods

Cell cultures

N2a murine neuroblastoma cells were grown in Dulbecco's modified Eagle's medium (DMEM)/Opti-MEM (1:1), 5% fetal bovine serum (FBS) and antibiotics. N2a cell differentiation was initiated by serum withdrawal and the addition of the indicated drug. Hippocampal neurones were isolated from embryonic day-17 rat embryos (E17 cells) by a modification of the method described by Wang *et al.*, (2002). Primary E17 cells were isolated from dissected hippocampi that were transiently maintained in Hanks' balanced salt solution. Five hippocampi were incubated with 0.25% trypsin/1 mM EDTA (Gibco-25200-056) for 24 min at 37°C. The medium was aspirated and the tissue was incubated for 10 min at 37°C in 10 mL A-DMEM/5% calf bovine serum, washed twice with Hanks buffered salt solution and dispersed mechanically (not more than 10 cycles) using a fire-polished Pasteur pipette. Hanks solution (5 mL) was added and cells were additionally dispersed with a Pasteur pipette. After resting the suspension for 10 min at room temperature, the supernatant was transferred to a 15 mL Falcon tube and centrifuged for 1 min × 800× *g*. The pellet was suspended in DMEM : F12 (1:1) medium/10% FBS and cells were counted in a Neübauer chamber. An intermediate density of viable cells (~8000 cells·cm^{-2}) were plated onto a P60 Petri dish containing poly-L-lysine-coated coverslips and incubated at 37°C in DMEM : F12 : FBS in a humidified 5% CO_2 atmosphere. Cultures were enriched for neurones by removing the plating medium after 2 h and replacing it with Neurobasal medium (Invitrogen, Argentina) supplemented with 2% B27 and 2 mM L-glutamine (referred to as 'culture medium' hereafter). Astrocyte isolation was performed as described by McCarthy and de Vellis, (1980), with 98% purity of viable cells.

Transfections

Overexpression of FKBP52 or GFP-tubulin was achieved by transfection of 1 μg DNA per well of 35 mm of pCI-Neo-hFKBP52 or pEGFP-C1-α-tubulin, respectively, following the calcium phosphate precipitation standard method (Gallo *et al.*, 2007). Controls were transfected with empty vector.

Interference of FKBP52 expression was achieved by transfection of a specific siRNA (or a scrambled siRNA) with the si-Importer transfection reagent for RNA (Upstate) according to the manufacturer's instructions.

Neurite outgrowth quantification

Neurite length was measured using the IMAGE Pro Plus 5.1.0.20 program (Media Cybernetics Inc., Bethesda, MD, USA) in those plate fields that showed lower cell density. For the spectrophotometeric measurement of axonal protoplasm, primary E17 cells were grown for 12 days using transwell cell culture inserts containing a permeable collagen-coated PTFE membrane with 3 μm pores at its base (Corning Inc. Life Sci., Lowell, MA, USA). FK506 was added to the receiver chamber filled with culture medium. After 14 days, inserts were washed with saline-phosphate buffer and cells were fixed for 20 min with methanol at room temperature. Cells were stained for 2 min with 0.1% Crystal Violet in saline buffer containing 7% methanol. After washing off excess Crystal Violet, the lower face of the transwell insert (for axons) or the upper face (for cell bodies) were incubated for 5 min on a layer of 200 μL of extraction buffer (0.2 M acetate at pH 4.5 with 50% methanol). Absorbance at 562 nm was measured against blanks made from transwell inserts containing no cells. For Western blot analyses, both cell bodies retained on the top of the membranes and the neurites that had traversed the pores were harvested by scraping the membrane and the proteins resolved by SDS-PAGE.

Indirect immunofluorescence assays

Cells grown on poly-lysine-coated coverslips were fixed and permeabilized as described previously (Quintá *et al.*, 2010). Fluorescence microscopy was performed with a Karl Zeiss LSM10 Meta confocal microscope (Göttingen, Germany). Image analyses for co-immunolocalizations were carried out using the (3D) surface plot plug-in of the IMAGEJ program (v.1.45) from the NIH (National Institutes of Health, Bethesda, MA, USA). 3D images were obtained from z-stack scanning of cells at a slice distance of 1.0 μm using the IMARIS 6.3.1 program (Bitplane Sci Software, Zürich, Switzerland). Axotomy was achieved by using a two-photon microscope Karl Zeiss LSM710 with exposure of cells for 20 s at 950 nm beam at its highest potency. The axon was identified through the stack as the only process with axonal morphology emerging from the cell body. To prevent damage of the cell body, the cut with the high energy beam was focused at a distance equivalent or slightly longer than those of the other processes.

All bars depicted in the Figures showing cells, represent a distance of 10 μm.

Data analysis

All experiments were repeated at least four times. Where it is indicated, results show the mean value ± SD. Different conditions were compared by unpaired Student's *t*-test performed using the GRAPHPAD PRISM program (v.5.0) (GraphPad Software Inc., La Jolla, CA, USA), and the significance level was set at $P = 0.05$.

Materials

All culture media were from Invitrogen-Life Technologies (Carlsbad, CA, USA). Phalloidin was from Sigma Chemical Co. (St. Louis, MO, USA). Bovine calf serum was from Internegocios (Mercedes, Argentina). FK506 was purchased from LC Laboratories (Wobrun, MA, USA). The JJ3 mouse monoclonal IgG against p23 was from Affinity BioReagents (Golden, CO, USA). The purified UP30 rabbit antiserum against FKBP52 and the 8D3 mouse monoclonal IgM were kind gifts from Dr William Pratt (University of Michigan). The A3S rabbit monoclonal IgG against histone H3 was from Upstate (Temecula, CA, USA). The TUJ1 mouse monoclonal IgG_{2a} against neuronal class III β-tubulin was from Covance (Emeryville, CA, USA). Mouse monoclonal IgG_1 against synapsin-1 was from Synaptic Systems (Göttingen, Germany). The GA5 mouse monoclonal IgG against glial fibrillary acidic protein (GFAP) was from Cell Signaling (Boston, MA, USA). The RMO-270 mouse monoclonal $Ig_{2a\text{-kappa}}$ anti-neurofilament-M (160 kDa) was from Invitrogen. Secondary antibodies labelled with Alexa-Fluor Dyes (488, 546 and 647) and 4′,6-diamidino-2-phenylindole (DAPI) were from Molecular Probes (Eugene, OR, USA). Goat anti-mouse IgG_1-Cy2 or anti-mouse IgG_{2a}-Cy3 were from Jackson ImmunoResearch (WestGrove, PA, USA). Horseradish peroxidase-conjugated goat anti-rabbit was from Pierce (Rockford, IL, USA) and the horseradish peroxidase-conjugated donkey anti-mouse was from Sigma Chemical Co.

Results

FK506-dependent differentiation of neuroblastoma cells

Undifferentiated N2a neuroblastoma cells in culture medium lacking serum were stimulated with FK506 without the addition of other trophic factors. The drug restricted cell division and produced profound morphological transformations in the cells, which became bipolar a few minutes after the stimulation and showed incipient neurites as soon as 2–3 h, after the addition of FK506 (Figure 1A). One day after FK506, the originally rounded cells showed the typical phenotype of a neuronal cell. More interestingly, the chaperone heterocomplex containing FKBP52, Hsp90 and p23, which was originally concentrated in the perinuclear area of undifferentiated cells, was rapidly dispersed into the cytoplasm of the cells, showing no obvious structure, when the differentiation programme was triggered by FK506. While control cells did not show any change after addition of the vehicle (0.01% v/v DMSO), the neurite length increased significantly in an FK506- and time-dependent manner (Figure 1B). The maximum effect was observed for 1 μM FK506 at all incubation times. Even though the effect was almost maximal after 0.1 μM FK506, for further experiments, 1 μM FK506 was used to make sure that during the incubation time no variations were observed in the cells due to the eventual metabolism or decay of the drug.

The phenotypic changes of this cell line match exactly those of natural neurones, including the induction and accumulation of neurofilament M in axons (Figure 1C). Studies of neurofilament transport in cultured neurones and computational modelling studies of neurofilament transport *in vivo* have demonstrated that they show rapid, but intermittent, movement along the axons interrupted by prolonged pauses (Trivedi *et al.*, 2007; Alami *et al.*, 2009), which makes them to accumulate in patches, as those seen in Figure 1C. A

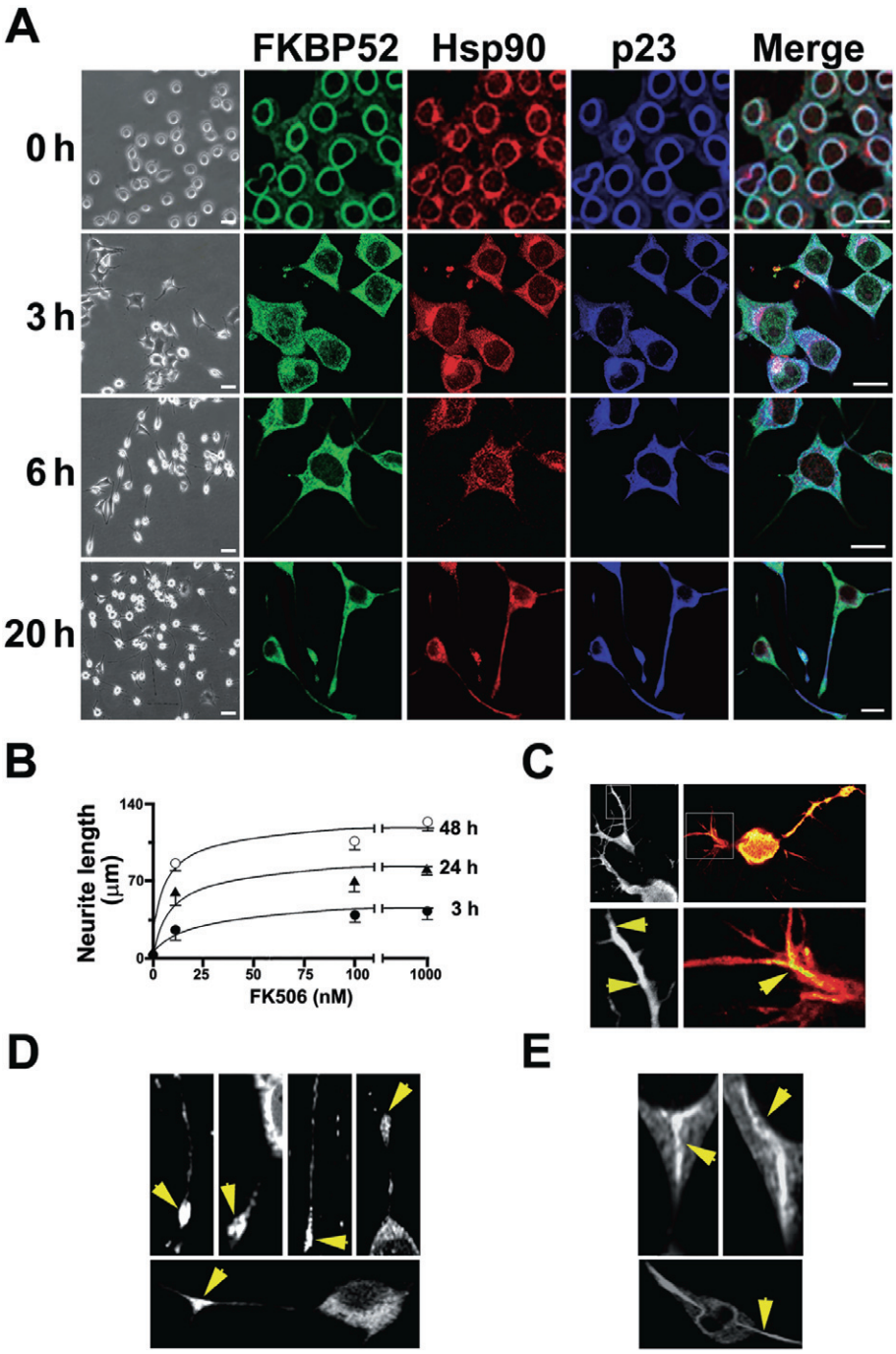

Figure 1

Differentiation of neuroblastoma cells induced by FK506. (A) N2a cells treated with 1 μM FK506 for the indicated times and were observed by phase contrast light microscopy (left column) or by confocal microscopy after performing an indirect immunofluorescence for FKBP52 (green), Hsp90 (red) and p23 (blue). (B) The neurite length was measured after 3 h, 24 h and 48 h of treatment with the indicated concentration of FK506. Results are shown as mean ± SD for more than 100 cells for each condition. (C) N2a cells develop neurites showing the typical growing gaps of neurofilament M observed in ganglia neurones (see arrows in the magnified areas of the bottom part). The coloured picture emphasizes the higher fluorescent signal in yellow on a red background. (D) Axon-like terminals showing the concentration of FKBP52 (arrowheads). (E) Magnification of p23 filaments after 3 h of differentiation with FK506.

computer-generated image using the Lut function of the Fiji image processing software clearly shows those gaps in yellow due to an increased number of pixels on the red background given by neurofilament M.

Regarding the redistribution of the chaperone complex, it should be noted that FKBP52 concentrated in terminal axons and ramification bodies (Figure 1D), whereas p23 was associated with the growing filaments that were to be part of

the axon-like neurites (Figure 1E). These events may be related to the early steps of the differentiation process in which the cytoskeletal architecture must be remodelled as a necessary event to allow the neurite extension. These observations are in agreement with a recent report (Quintá *et al.*, 2010) and with those studies where it was suggested that TPR-domain immunophilins and the Hsp90-based complex are required for remodelling the architecture of cytoskeletal structures (Czar *et al.*, 1996; Galigniana *et al.*, 2002; Chambraud *et al.*, 2007; Inberg *et al.*, 2007; Abisambra *et al.*, 2010).

Even though it is likely that all three proteins formed a heterocomplex in the perinuclear rings, such structures rapidly disassembled when the cells were treated with FK506. Figure 2A shows that such rearrangement of chaperones is sequential as p23 (blue) abandons the annular structure at a lower rate than FKBP52 (green) and Hsp90 (red). This is more clearly seen in the magnified cell of Figure 2A and the colour profile plot shown under the cell, where FKBP52 and Hsp90 form a merged yellow ring structure dissociated from the blue inner ring of p23. The bar graph in Figure 2B demonstrates that there are a number of cells showing a partial ring after 3 h with FK506, a condition where cells showing full rings decreased to 25% (vs. 95% in the undifferentiated state). While the differentiation process proceeds, a minimal number of cells, if any, show the annular structure of chaperones after 6 h of treatment, including the slower migrating co-chaperone p23. This particular rearrangement of proteins belonging to the immunophilin•Hsp90 complex is not a general event for all proteins primarily located in the nucleus. Thus, cyclophilin A (CyPA), another member of the immunophilin family that is unable to bind FK506, remained entirely nuclear after a 3 h of treatment with FK506 in the same cell where the perinuclear ring of Hsp90 has disassembled (Figure 2C).

The knock-down of FKBP52 with a specific siRNA prevented both the regular organization of Hsp90 and p23 in full nuclear rings (Figure 2D) and the proper growth of neurites (Figure 2E), whereas its overexpression favoured neurite outgrowth. Figure 2E shows that the length of neurites after 4 h of treatment with FK506 was greatly increased, compared with control cells. All these observations agree with the implied key role of FKBP52 in the formation of the annular structures and its concentration in terminal axons and ramification bodies.

FK506-dependent differentiation of hippocampal neurons

The events described above were not due to the particular properties of a given cell line. Figure 3A demonstrates that chaperones also form the same annular structures that disassemble upon stimulation with FK506 in hippocampal neurones isolated from 17 day rat embryos. As observed with N2a cells, a high percentage of hippocampal cells treated with the drug also show FKBP52 concentrated in the growth cones of outgrowing neurites and at the nascent ramifications sites. However, in contrast to N2a cells, which show an absolute requirement for FK506 in the medium to differentiate, E17 cells can evolve into neurones over time, even in the absence of drug, although this evolution occurred at a slower rate than in its presence and also generated shorter axons. As an example, 72 h after the addition of FK506 to the medium, the average neurite length was significantly greater ($P < 0.001$) than in spontaneously differentiated cells (180 ± 10 μm vs. 80 ± 8 μm).

Figure 3B shows that, in contrast to the annular structure shown by undifferentiated E17 cells, the distribution of FKBP52 (green) is mainly cytoplasmic in embryonic neurones cultured *in vitro* for 3 or 13 days, although the presence of FK506 makes FKBP52 more axonal in the latter case (Tau1 is shown in red and actin in blue). More interestingly, when the axons of the cells were damaged with the tip of a needle and cells were kept in culture to allow regeneration, FKBP52 cycled back to the nucleus, the immunophilin being more cytoplasmic in those cells treated with FK506 than in cells reincubated without the drug. This is shown in the 20 DIV panel, where E17 cells have been counter-stained for β_{III}-tubulin to show more clearly the localization of FKBP52 in both axons and dendrites. Note in the same field the presence of two contaminant glial cells where FKBP52 is nuclear and cytoplasmic, but the phenotype of these cells is clearly different from that of neurones and they are negative for β_{III}-tubulin staining.

Even though FKBP52 cycled back to the nucleus in E17 cells, its pattern in the organelle was diffuse rather than concentrated in any particular structure, such as the ring observed in the undifferentiated state. Nonetheless, the continuous presence of the differentiating agent also preserved FKBP52 in the rest of the neuronal structures, which could be related to its potential need for remodelling the cytoskeletal architecture. More importantly, these experiments showed that the properties of hippocampal neurones and neuroblastoma cells were comparable, the latter being a system where the potential influence of glial cells in the medium is clearly lacking.

Subcellular redistribution of the FKBP52•Hsp90•p23 complex in astrocytes

Our results show that the FKBP52•Hsp90•p23 complex moved in a sequential manner from perinuclear areas to the cytoplasm of neurones stimulated with FK506. This particular rearrangement of the chaperone complex was not observed in other somatic cell types treated with FK506 or other specific differentiating agents (e.g. differentiation of fibroblasts to adipocytes). Therefore, we asked whether the FK506-dependent relocalization of the heterocomplex also takes place in other cells of the nervous tissue. Consequently, the subcellular localization of the chaperones was analysed in astrocytic glial cells isolated from cerebral cortices of 2-day-old rat neonates. Figure 4A shows that FKBP52 is primarily nuclear in flat polygonal type I astrocytes, but this nuclear localization does not show the particular subnuclear distribution observed in neurones. Figure 4B shows the differential localization for FKBP52 (mostly nuclear) and Hsp90 (mostly excluded from nuclei) in protoplasmic-like astrocytes counter-stained for GFAP. Due to incompatibility of antibody species, p23 must be assayed separately in cells counter-stained for actin with phalloidin (Figure 4C), and showed similar localization to FKBP52. This distribution of p23 in glial cells is different from that described for mature neurones, where the co-chaperone co-localizes with neurofilaments (Quintá *et al.*, 2010). Figure 4D shows FKBP52 in a

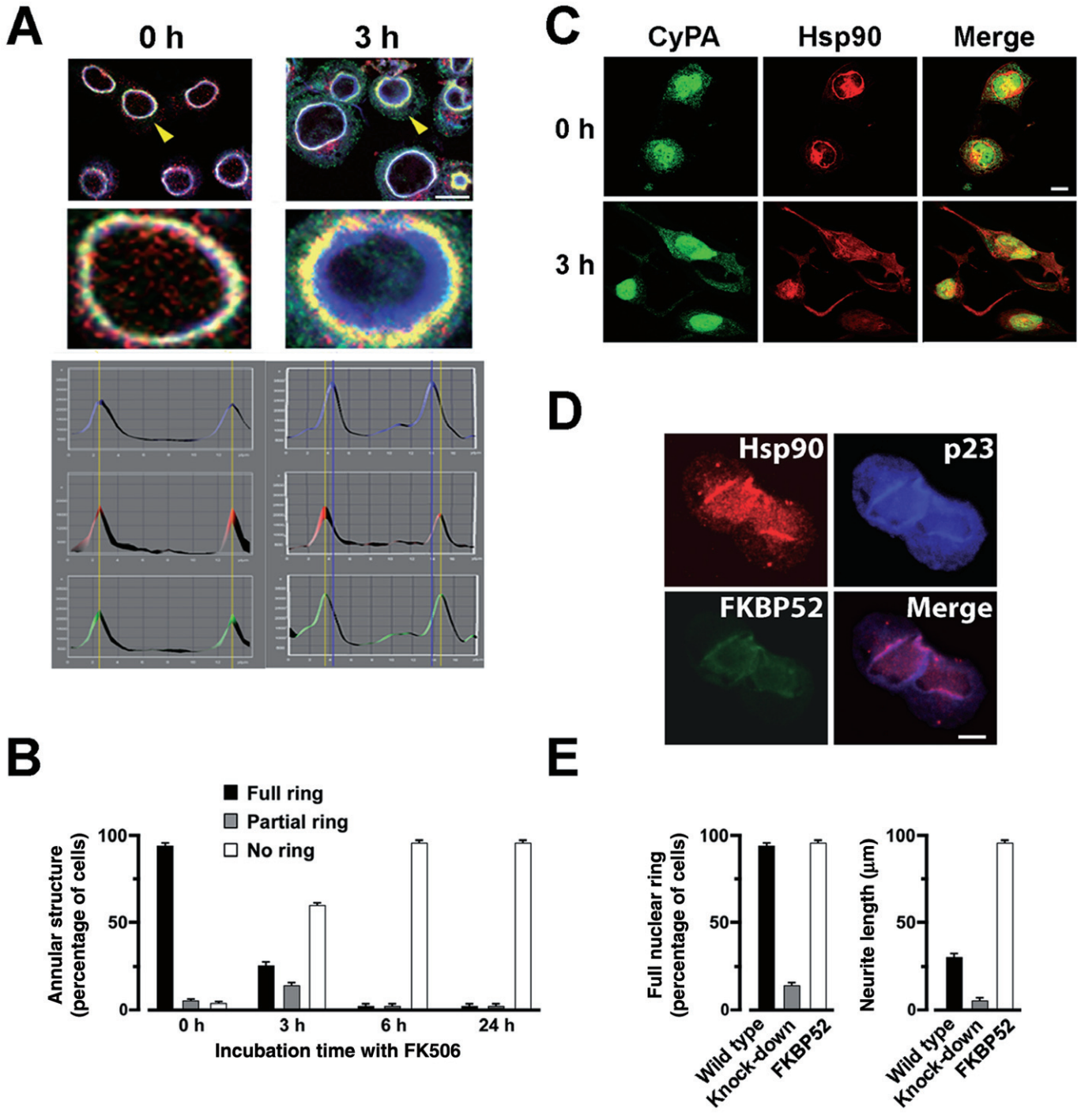

Figure 2

Early sequential disassembly of the annular structure. (A) N2a cells were treated with FK506 for 3 h. The subcellular localization of FKBP52 (green), Hsp90 (red) and p23 (blue) is shown. Note that after 3 h with the drug, FKBP52 and Hsp90 (yellow ring) have started to migrate towards the cytoplasm, whereas p23 is still in place. (B) The bar graph shows the number of cells showing full, partial and no annular structures during the incubation with FK506 (mean ± SD, $n = 100$ cells). (C) Subcellular localization of CyPA remains unchanged in the same cell where Hsp90 was redistributed during the early steps of differentiation. (D) Hsp90 and p23 are not organized in annular structures in undifferentiated cells where FKBP52 was knocked-down. (E) The expression of FKBP52 influences both the formation of perinuclear rings (left bar graph) and the neurite length (right bar graph). N2a cells were stimulated with FK506 for 4 h (wild type) or treated with an siRNA against FKBP52 (knock down) or transfected with pCI-Neo-hFKBP52.

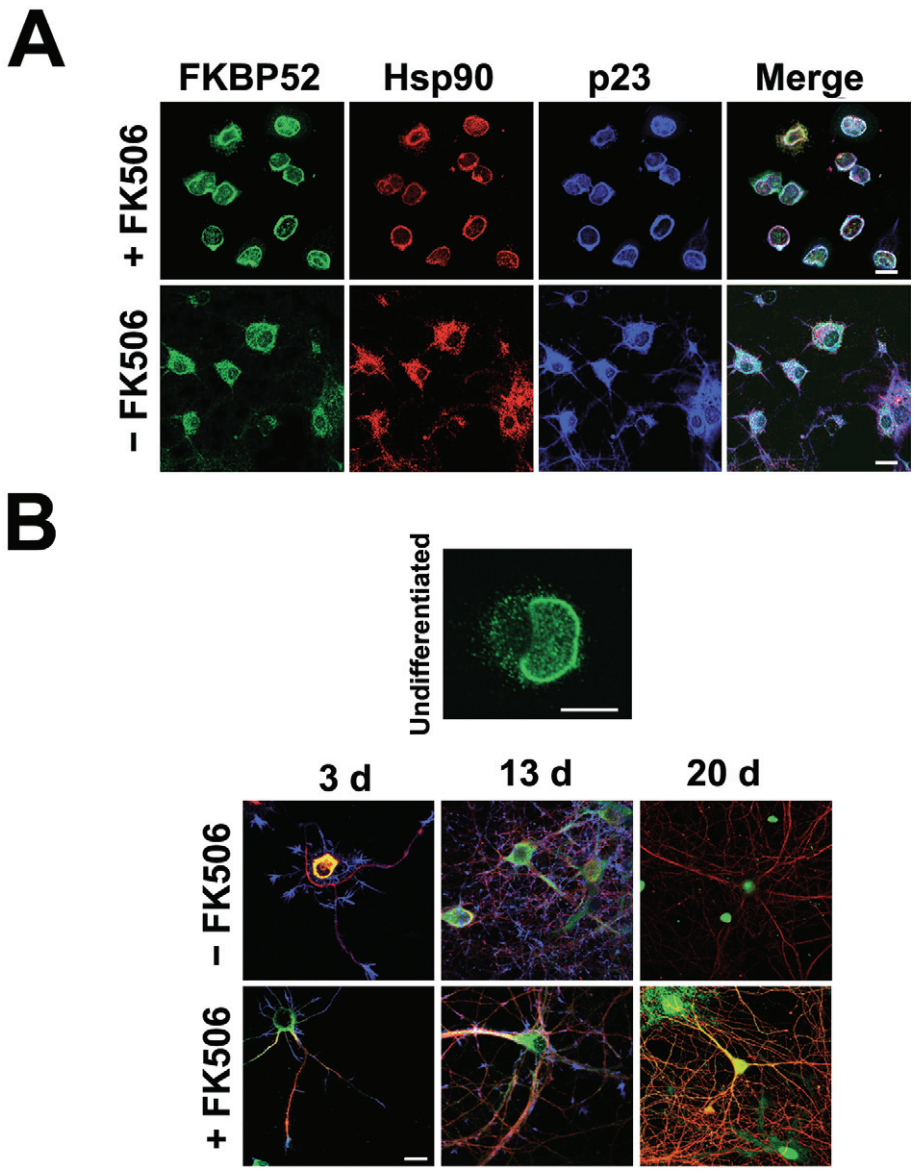

Figure 3

Differentiation of hippocampal neurones induced by FK506. (A) Hippocampal neurones were isolated from embryonic day-17 rat embryos. Undifferentiated cells show an annular pattern of chaperones, identical to those in the neuroblastoma cell line (FKBP52, green; Hsp90, red; p23, blue) and spread out through the cytoplasm in the presence of 1 μM FKBP506. (B) E17 cell differentiation to neurones takes place even in the absence of FK506 (*-FK506*), although FKBP52 (green) is not localized with the axonal marker Tau1 (red) as in FK506-traeated cells (*+FK506*). Note that from day 3 to day 13, FKBP52 has expanded to axons in both treated and untreated cells, but co-localization with Tau1 is stronger in FK506-treated cells. The last panel shows neurones where axons were cut with the tip of a needle and then reincubated with and without the drug after washing out the debris. Note that FKBP52 cycled back to the nucleus of E17 cells, but it is still axoplasmic in FK506-treated cells. These cells were counterstained for β_{III}-tubulin (red) to better visualize the entire cytoskeleton.

wide field of FK506-treated cells where a neuronal body is seen (see arrowhead and the black and white magnification on the right panel). Clearly, the immunophilin is located in different compartments in both cell types of the same field. Therefore, the atypical arrangement of chaperones in the internal border of the nucleus and their ability to migrate after triggering the differentiation programme seem to be an exclusive phenomenon of neuronal cells.

Subcellular relocalization of the FKBP52•Hsp90•p23 complex in injured neuroblastoma cells

Next, we asked whether the assembly and disassembly events of the FKBP52•Hsp90•p23 heterocomplex were necessary for the first step of the differentiation programme that commits the cell to become a mature neuron. Therefore, N2a cultures

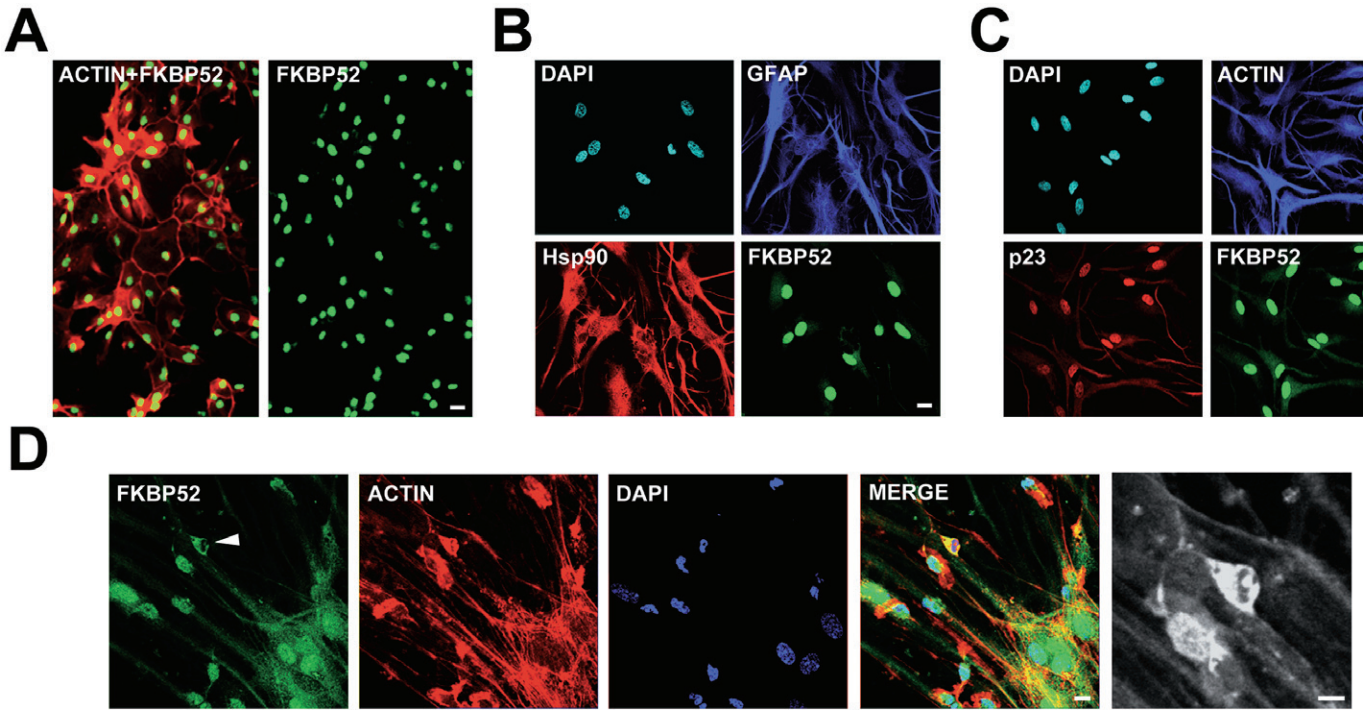

Figure 4

Subcellular localization of chaperones in astrocytes. (A) Polygonal type I astrocytic glial cells isolated from cerebral cortices of 2-day-old rat neonates show FKBP52 (green) concentrated in nuclei (cells were counterstained with phalloidin). The same localization was observed after cell treatment with FK506 (data not shown). (B) Indirect immunofluorescence for FKBP52 (green) and Hsp90 (red) in protoplasmic-like astrocytes counter-stained for glial fibrillary acidic protein (GFAP; blue). (C) Indirect immunofluorescence for FKBP52 (green) and p23 (red) in the same cells, but counterstained with phalloidin (blue). (D) FK506-treated astrocytes where a contaminant neuronal body is shown by an arrowhead (black and white magnification on the right). Note that FKBP52 is cytoplasmic rather than primarily nuclear, as it is seen in all astrocytes.

were damaged with the tip of a sterile needle following a squared pattern to make sure that all axon-like extensions were cut. After checking the plate under the microscope to evaluate the efficiency of the mechanical damage, the medium was changed to remove debris and cells were incubated for 3 h to allow them to recover. Then, cells were fixed or reincubated with 1 μM FK506 for different periods of time before fixation. Figure 5A shows the cells before (Pre) and after (Post) scratching the plate. Confocal microscopy images show that the damaged cells recovered the original round shape already observed in undifferentiated cells. Strikingly, all three proteins FKBP52, Hsp90 and p23 reorganized in an annular structure. After a few hours, the proteins migrated to the cytoplasm and they adopted exactly the same pattern as that shown before the injury in the differentiated neuron, including the accumulation of FKBP52 in terminal axons surrounded by Hsp90 and p23 (Figure 5B). More interestingly, those cells showing a delayed response (indicated by arrowheads) still preserved the annular structure of chaperones.

Even though all treated cells developed axons after the mechanical damage, we assessed whether the chaperone redistribution was associated with early steps of the neuroregeneration process or with cell death. Those cells stimulated with FK506 showed perinuclear rings of Hsp90 (Figure 5C). In contrast to the aspect of apoptotic nuclei observed in Annexin V-stained positive control cells, all injured cells treated with either DMSO or FK506 showed normal distribution of chromatin, confirming that the redistribution of chaperones was related to the regeneration process, rather than a cell death process.

A clear demonstration that axons can be regenerated in injured cells was obtained in GFP-tubulin expressing cells whose axons were dissected with a laser beam and then incubated with FK506 for 4 h. Figure 5D shows that axon-like neurites were regenerated in the same injured cell. This observation agrees with studies where lesioned neurones were capable of regenerating axon-like structures, even from pre-existing dendrites opposing the original axon (Calderon de Anda *et al.*, 2008; Gomis-Ruth *et al.*, 2008).

Subcellular relocalization of the FKBP52•Hsp90•p23 complex in injured hippocampal neurons

The experiments described above clearly show that not only the events related to neuronal differentiation involved the rearrangement of the chaperone complex in nuclear structures but also the process of neuroregeneration after a mechanical injury. In order to test this principle in primary cells, the experiment was repeated using isolated hippocampal neurons. Figure 6A shows that the cells have rearranged the chaperone heterocomplex in a perinuclear structure again. To test the effects of FK506 in axon regeneration, neurones were grown until they formed a tight monolayer. Then, cells were damaged with the tip of a sterile needle

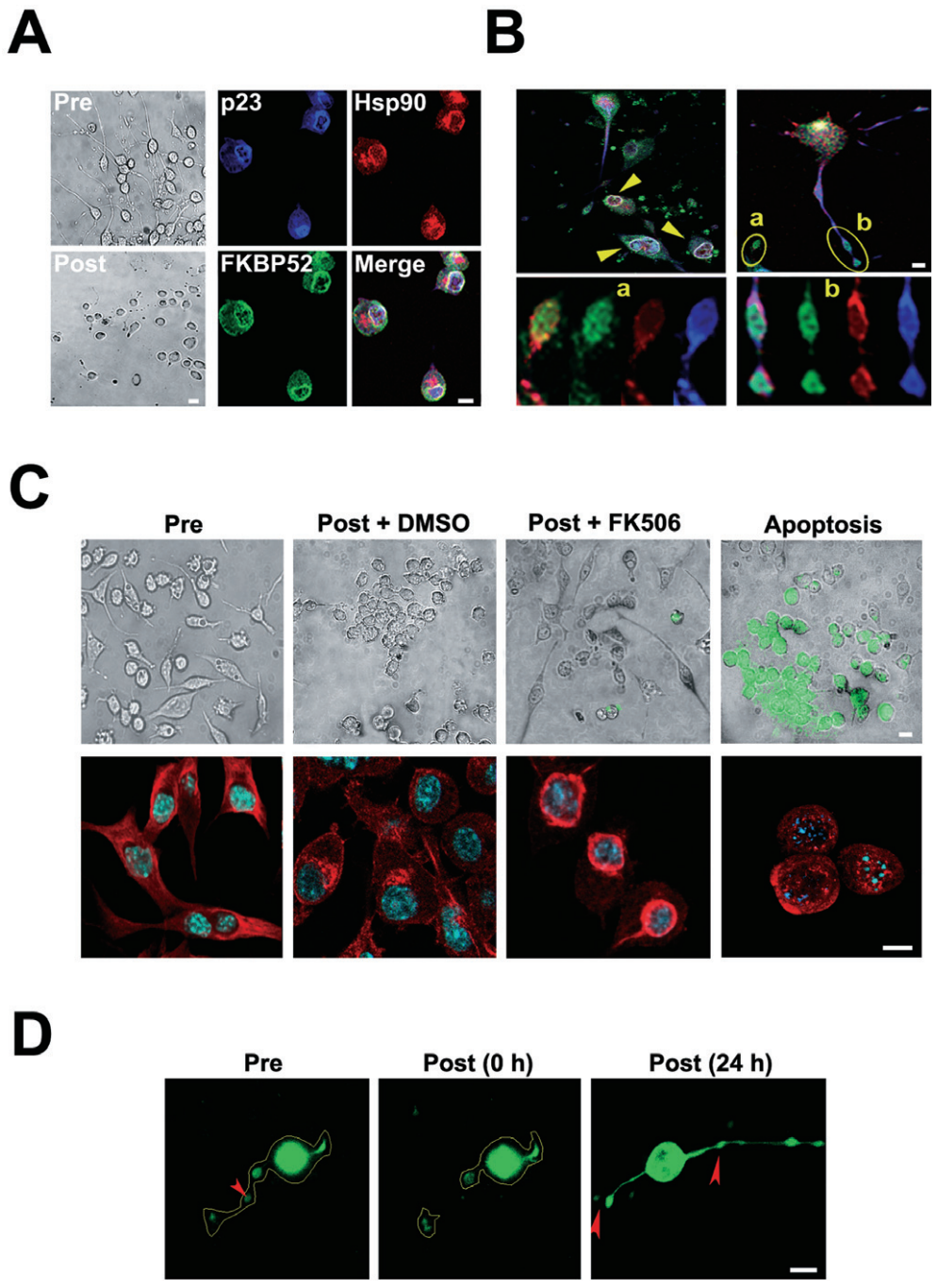

Figure 5

Relocalization of the FKBP52•Hsp90•p23 complex in injured neuroblastoma cells. (A) N2a cells were injured mechanically with a needle. After checking the damage with a microscope (left panels; before (Pre) and after (Post) scratching the plate), the medium was changed to remove debris and cells were incubated with 1 μM FK506 for 3 h to allow them to recover. The right panel shows an indirect immunofluorescence by confocal microscopy for the three proteins of the heterocomplex. Note that the chaperones have reorganized in perinuclear structures. (B) When these damaged cells were reincubated with FK506, neuron-like cells were observed after 24 h. Note that those cells exhibiting a slower rate of differentiation to neuronal phenotype still show perinuclear structures (arrowheads), whereas those that exhibit a neuron-like phenotype show Hsp90 and p23, delimiting a concentrated central area of FKBP52 in terminal axons (panels A and B are magnifications of the corresponding circled areas). (C) Apoptotic cells do not reorganize the chaperone complex. Damaged N2a cells cycled Hsp90 (red) back to the nucleus in the presence of FK506 only. The number of apoptotic cells is not high after 4 h after the damage (as it is shown by FITC-Annexin V-staining and Hoechst-stained nuclear bodies). Note that the chaperone follows no pattern in apoptotic cells. (D) Proximal axotomy of a neuron shows high cell transformation plasticity. The proximal extreme of an axon-like neurite of a cell transfected with GFP-tubulin was exposed to a high intensity beam at 950 nm for 30 s in a two-photon excitation microscope (Pre, see arrowhead). The middle panel shows the same treated cell after the cut (Post 0 h). This cell was incubated with 1 μM FK506 and visualized after 4 h (Post 4 h). Arrowheads show the newly generated neurites.

Figure 6

Heterocomplex rearrangement in damaged E17 hippocampal neurones. (A) E17 cells were grown until they formed a tight monolayer. Then, cells were subjected to a wound-healing treatment with the tip of a needle, washed and fixed after 3 h of incubation. Note that the FKBP52•hsp90•p23 complex is rearranged in a perinuclear ring. (B) The wounded preparation of cells was incubated with 1 μM FK506 for 24 h (middle panel) and controls were incubated with the vehicle (left panel). Cells were fixed and stained for FKBP52 (green) and β_{III}-tubulin (red). The lower left panel and the upper right panel show a magnification of the dashed boxes. Note the presence of the newly generated axons in FK506-treated cells and the distribution of FKBP52 in these cells compared with those cells not stimulated with the drug. (C) Indirect immunofluorescence showing the subcellular localization of FKBP52 in cells incubated with or without FK506. The right panels show a 3D computer-generated image of the cells shown in the inset. Note the spreading of FKBP52 in axons and the increased branching exhibited by FK506-treated cells. (D) E17 cells were grown on transwell cell culture inserts as described. After 12 days, the axons that had traversed towards the lower face of the porous membrane were extracted (Pre). Cells were incubated with 1 μM FK506 for 14 days and the newly generated axons were extracted again (Post). The upper panel shows a Western blot for the latter lysates (two independent samples). Histone H3 was used as a marker of cell bodies (*Lower* and *Upper* refer to the side of the porous membrane where protoplasm was obtained). The bar graph shows a quantification of the axonal mass of protoplasm by using a Crystal Violet assay (*$P < 0.001$). (E) E17 cells treated as described for panel B were stained for synapsin-1 (green) and β_{III}-tubulin (red). Note the yellow merged spots in the newly generated axons crossing the wound.

generating a protoplasm-free 'wound' that simulates a channel among the cells. Cells were then incubated with the vehicle (upper-left image in Figure 6B, see the magnified area immediately below) or 1 μM FK506 for 24 h (middle mounted image showing two consecutive fields). Two major events were noted: (i) a number of newly generated axons crossing the wound (see the magnified area on the upper-right corner of the panel and the bar graph on the lower right corner corresponding to a section length of 3500 μm) and (ii) the yellow colour shown by all cells, indicating the massive migration of FKBP52 (green) in cells counterstained for β_{III}-tubulin (red). Such differential distribution of FKBP52 was also shown in Figure 6C and clearly mimicked the primary events observed for normal cells during the early differentiation process (Figures 1 and 3). The right-hand side image of panel 6C is a computer-generated 3D image from a *z*-stack scanning of single neurones showing the FK506-dependent cytoplasmic dispersion of FKBP52 after the injury (the original cells are shown in the inset).

Then, E17 cells were grown for 12 days on transwell cell culture inserts containing a permeable membrane with 3 μm pores at its base, through which axons traverse towards the lower face of the membrane. Axons were sliced and the inserts were reincubated with FK506 for 2 weeks. Lysates of the upper (somas) and lower (axons) faces of the membrane were resolved by Western blotting to confirm the presence of FKBP52 (top of Figure 6D), with β_{III}-tubulin being used as a neuronal marker and histone H3 as a cell body marker. Note that H3 was detected in lysates obtained from the upper layer of the membrane only, indicating that there was no contamination of the axonal preparation with cell bodies. In turn, the amount of axonal mass was assayed by the Crystal Violet test (bar graph) and showed that axons were almost completely regenerated after 2 weeks of treatment with FK506.

Finally, we asked whether the newly regenerated axons can form synaptic clusters, so the wound-healing experiment described in Figure 6B was repeated and an indirect immunofluorescence for synapsin-1 was performed. Figure 6E clearly shows the presence of this presynaptic marker in the newly generated axons in cells treated with FK506. As it is known that a fraction of newly synthesized synapsin-1 is axonally transported at the velocity of the most rapidly transported proteins and comprise membrane-associated proteins and elements of synaptic vesicles (Baitinger and Willard, 1987), this observation suggests that the regenerated axons could be functionally active, at least regarding protein and vesicle trafficking.

Discussion

This study suggests a close relationship between the disassembly of the FKBP52•Hsp90•p23 chaperone complex in the nucleus and the progression of both differentiation and regeneration. During the early steps of differentiation, the chaperones migrate from a perinuclear arrangement to the cytoplasm. They become associated with cytoskeletal structures and active axonal areas such as terminal ends and branching bodies. More importantly, in this work, when the axons of differentiated neurones were cut, the chaperones reorganized back to perinuclear structures, similar to those originally observed in undifferentiated cells. This suggests that this type of nuclear arrangement must precede the neuroregeneration process after the injury. In other words, this study suggests that both processes, neurodifferentiation and neuroregeneration, appear to be mechanistically linked to the FKBP52•Hsp90•p23 heterocomplex.

Regarding the organization of those three proteins, co-immunoadsorption assays performed with undifferentiated neuronal lysates have shown that they do form a complex (data not shown). This is expected according to a number of previous studies from several laboratories (Kanelakis *et al.*, 2000; Felts and Toft, 2003; Pratt *et al.*, 2004; Davies *et al.*, 2005; Picard, 2006; Cox *et al.*, 2007; Galigniana *et al.*, 2010b). Nonetheless, this assay cannot distinguish between complexes normally present in cytosol and nucleoplasm, from those located in the perinuclear structure. Even so, there is no reason to think that the chaperones cannot form a complex in the ring of undifferentiated neurones as the three purified proteins are capable of assembling spontaneously in a medium containing buffer only (Murphy *et al.*, 2003). Moreover, the use of an antibody (clone Ac88) able to recognize free Hsp90 but not Hsp90 associated with complexes did not show the chaperone in a perinuclear ring (Quintá *et al.*, 2010). However, the differential rate of migration observed in neurones for the three chaperones during the early steps of differentiation suggests that the original nuclear heterocomplex should be disassembled during the differentiation process.

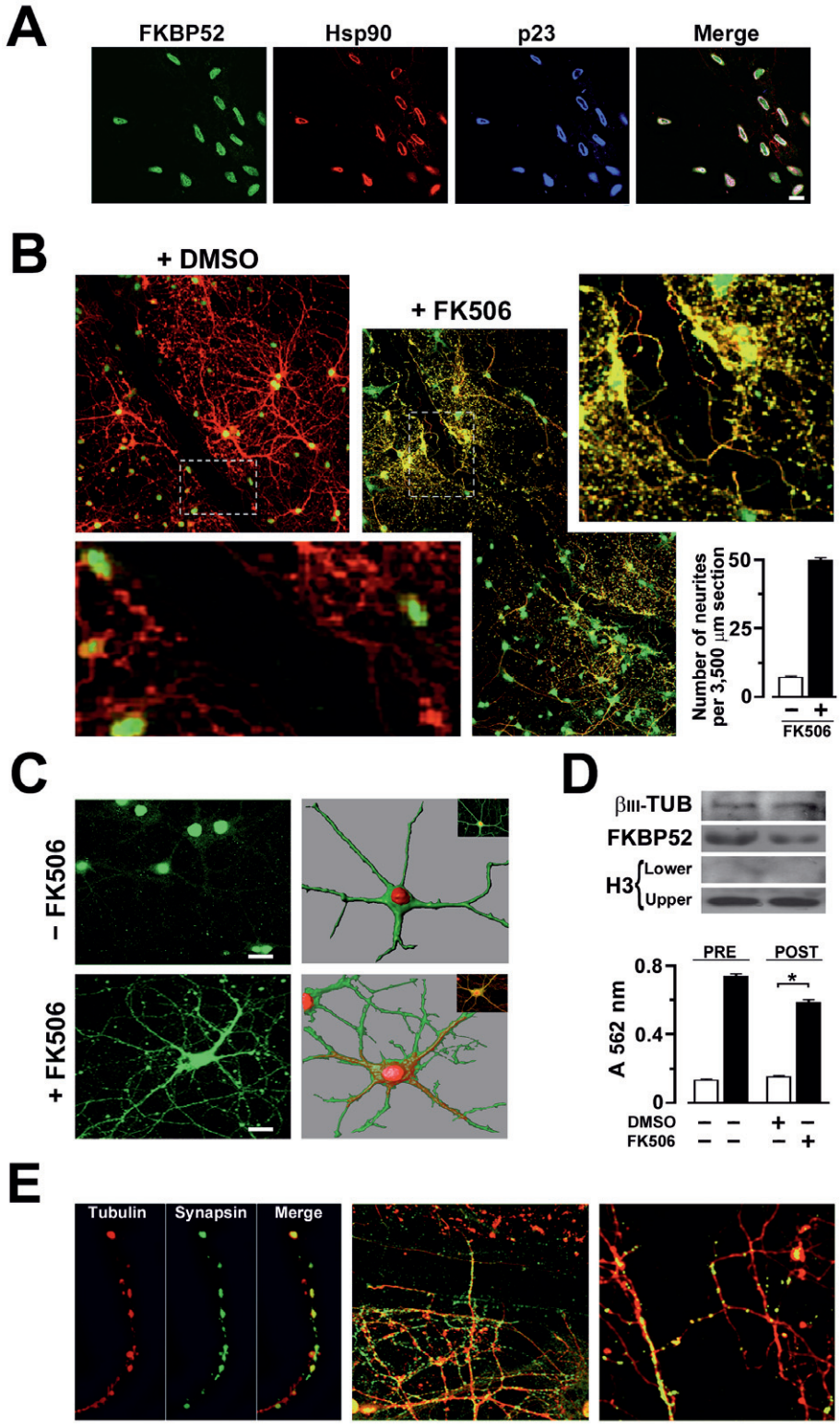

N2a neuroblastoma cell line and embryonic hippocampal E17 neurones provide excellent models to study the molecular programmes of differentiation and regeneration. Both cell types are alike and share the most important steps of both processes studied here. More importantly, N2a cells show accumulation of neurofilament N in the growing axon (Figure 2C), as described for neurones (Trivedi *et al.*, 2007; Alami *et al.*, 2009). Also, they are easier to synchronize than primary cultures and show higher transfection efficiency for plasmids encoding immunophilins or siRNAs. In contrast to N2a cells, E17 cells show a high rate of spontaneous differentiation over time (see Figure 3B), perhaps due to the stimuli that these cells are exposed *in vivo*, compromising the progression of the differentiation programme. Even so, in these cells,

the events are always faster and more efficient when FK506 is added to the medium. Studies shown in Figures 1 and 2 confirm our recent work on the properties of the chaperone system during neuronal differentiation (Quintá *et al.*, 2010) and also expand those observations supporting the relevance of the N2a cell line as a model, equivalent to primary neurones, for the study of the neuronal differentiation process.

It is important to emphasize that FKBP52 (but not Hsp90 and p23) returned to the nucleus after axotomy (Figures 3 and 6). However, the distribution of the immunophilin in the nucleus of differentiated cells was totally different from that observed in undifferentiated cells. It may be that the peculiar organization of the FKBP52•hsp90•p23 complex in the nucleus may shape the architecture of chromatin, affecting the expression of key genes required for the differentiation programme. According to this interpretation, these perinuclear areas acquire high transcriptional activity in the presence of FK506 (Quintá *et al.*, 2010). Moreover, recent evidence indicates that the periphery of the nucleus provides a platform for sequestering transcription factors away from chromatin when these factors interact physically with components of the inner membrane (Heessen and Fornerod, 2007). Thus, it has been proposed that the nuclear periphery is a highly dynamic compartment able to undergo epigenetic regulations. This could be the case for the differentiation/regeneration programme and the heterocomplex of chaperones could influence this mechanism.

There are examples in other systems that support the hypothesis that the mechanism of regeneration process for neurones could resemble the early steps of differentiation. For example, heterokaryon formation between B lymphocytes and myocytes leads to the acquisition of myocyte properties in the B cell nuclei, which begins expressing muscle-specific genes (Terranova *et al.*, 2006). This clearly indicates that stimuli coming from the cell periphery (like an axotomy in neurons) affect the properties of the nuclear programme. Similarly, lymphocytes can be reprogrammed by injection into mouse oocytes (Hochedlinger and Jaenisch, 2002). More recently, neural progenitor cells of ectodermal lineage were reprogrammed into pluripotent stem cells, suggesting that *in vitro* reprogramming could be a universal process (Eminli *et al.*, 2008). Undoubtedly, a combination of factors is necessary for reprogramming the cell fate and this is dependent on the cellular context. In the case of damaged neurones, the process is triggered by cytoplasmic signals that are activated during the axonal injury. One of the early events associated with neuronal differentiation is the activation of the MAPK cascade (Price *et al.*, 2003; Gold and Zhong, 2004; Quintá *et al.*, 2010), although the mechanistic aspects are still unknown.

Even though FKBP52 appears to be a key factor for the early steps of the neurotrophic effect, the existence of viable and apparently normal mice with genetic deletion of this immunophilin, implies that FKBP52 is not essential for the development of the nervous system, which shows several redundant mechanistic pathways. However, whether or not FKBP52 is critical for the 'normal' development of the nervous system in many other aspects (e.g. learning, depression and anxiety) is a very different issue that should be addressed in further studies with those knockout models. In this study, FKBP52 was required for the efficiency of the very early steps (from minutes to a few hours) of the neurodifferentiation process. Moreover, such processes seemed to require the formation of particular arrangements of the immunophilin, together with Hsp90 and p23, in the nucleus.

We have earlier proposed that FKBP52 may control the neuronal programme of cell differentiation (Quintá *et al.*, (2010). The current study extends this concept to neuronal regeneration, implying that the elucidation of one mechanism may help to explain the other.

Acknowledgements

The authors are indebted to Dr William Pratt for the kind gift of the UP30 antibody against FKBP52 and the 8D3 antibody against Hsp90, and to Dr Marc Cox and Dr Alfreso Cáceres for sharing the plasmids encoding for FKBP52 and GFP-tubulin respectively. This work was supported by grants from the Agencia Nacional de Promoción Científica y Tecnológica de Argentina (PICT-2010/1170) and Programación Científica y Tecnológica de la Universidad de Buenos Aires (UBACYT-20020100100237).

Conflict of interest

None.

References

Abisambra JF, Blair LJ, Hill SE, Jones JR, Kraft C, Rogers J *et al.* (2010). Phosphorylation dynamics regulate Hsp27-mediated rescue of neuronal plasticity deficits in tau transgenic mice. J Neurosci 30: 15374–15382.

Alami NH, Jung P, Brown A (2009). Myosin Va increases the efficiency of neurofilament transport by decreasing the duration of long-term pauses. J Neurosci 29: 6625–6634.

Baitinger C, Willard M (1987). Axonal transport of synapsin I-like proteins in rabbit retinal ganglion cells. J Neurosci 7: 3723–3735.

Calderon de Anda F, Gartner A, Tsai LH, Dotti CG (2008). Pyramidal neuron polarity axis is defined at the bipolar stage. J Cell Sci 121 (Pt 2): 178–185.

Callebaut I, Renoir JM, Lebeau MC, Massol N, Burny A, Baulieu EE *et al.* (1992). An immunophilin that binds M(r) 90,000 heat shock protein: main structural features of a mammalian p59 protein. Proc Natl Acad Sci U S A 89: 6270–6274.

Chambraud B, Belabes H, Fontaine-Lenoir V, Fellous A, Baulieu EE (2007). The immunophilin FKBP52 specifically binds to tubulin and prevents microtubule formation. FASEB J 21: 2787–2797.

Cox MB, Riggs DL, Hessling M, Schumacher F, Buchner J, Smith DF (2007). FK506-binding protein 52 phosphorylation: a potential mechanism for regulating steroid hormone receptor activity. Mol Endocrinol 21: 2956–2967.

Czar MJ, Welsh MJ, Pratt WB (1996). Immunofluorescence localization of the 90-kDa heat-shock protein to cytoskeleton. Eur J Cell Biol 70: 322–330.

Davies TH, Sanchez ER (2005). Fkbp52. Int J Biochem Cell Biol 37: 42–47.

Davies TH, Ning YM, Sanchez ER (2005). Differential control of glucocorticoid receptor hormone-binding function by tetratricopeptide repeat (TPR) proteins and the immunosuppressive ligand FK506. Biochemistry 44: 2030–2038.

Echeverria PC, Mazaira G, Erlejman A, Gomez-Sanchez C, Piwien Pilipuk G, Galigniana MD (2009). Nuclear import of the glucocorticoid receptor-hsp90 complex through the nuclear pore complex is mediated by its interaction with Nup62 and importin beta. Mol Cell Biol 29: 4788–4797.

Eminli S, Utikal J, Arnold K, Jaenisch R, Hochedlinger K (2008). Reprogramming of neural progenitor cells into induced pluripotent stem cells in the absence of exogenous Sox2 expression. Stem Cells 26: 2467–2474.

Felts SJ, Toft DO (2003). p23, a simple protein with complex activities. Cell Stress Chaperones 8: 108–113.

Galigniana MD, Harrell JM, Murphy PJ, Chinkers M, Radanyi C, Renoir JM *et al*. (2002). Binding of hsp90-associated immunophilins to cytoplasmic dynein: direct binding and in vivo evidence that the peptidylprolyl isomerase domain is a dynein interaction domain. Biochemistry 41: 13602–13610.

Galigniana MD, Echeverría PC, Erlejman AG, Piwien-Pilipuk G (2010a). Role of molecular chaperones and TPR-domain proteins in the cytoplasmic transport of steroid receptors and their passage through the nuclear pore. Nucleus 1: 299–308.

Galigniana MD, Erlejman AG, Monte M, Gomez-Sanchez C, Piwien-Pilipuk G (2010b). The hsp90-FKBP52 complex links the mineralocorticoid receptor to motor proteins and persists bound to the receptor in early nuclear events. Mol Cell Biol 30: 1285–1298.

Gallo LI, Ghini AA, Piwien Pilipuk G, Galigniana MD (2007). Differential recruitment of tetratricorpeptide repeat domain immunophilins to the mineralocorticoid receptor influences both heat-shock protein 90-dependent retrotransport and hormone-dependent transcriptional activity. Biochemistry 46: 14044–14057.

Gold BG, Villafranca JE (2003). Neuroimmunophilin ligands: the development of novel neuroregenerative/neuroprotective compounds. Curr Top Med Chem 3: 1368–1375.

Gold BG, Zhong YP (2004). FK506 requires stimulation of the extracellular signal-regulated kinase 1/2 and the steroid receptor chaperone protein p23 for neurite elongation. Neurosignals 13: 122–129.

Gold BG, Densmore V, Shou W, Matzuk MM, Gordon HS (1999). Immunophilin FK506-binding protein 52 (not FK506-binding protein 12) mediates the neurotrophic action of FK506. J Pharmacol Exp Ther 289: 1202–1210.

Gomis-Ruth S, Wierenga CJ, Bradke F (2008). Plasticity of polarization: changing dendrites into axons in neurons integrated in neuronal circuits. Curr Biol 18: 992–1000.

Heessen S, Fornerod M (2007). The inner nuclear envelope as a transcription factor resting place. EMBO Rep 8: 914–919.

Hochedlinger K, Jaenisch R (2002). Monoclonal mice generated by nuclear transfer from mature B and T donor cells. Nature 415: 1035–1038.

Inberg A, Bogoch Y, Bledi Y, Linial M (2007). Cellular processes underlying maturation of P19 neurons: changes in protein folding regimen and cytoskeleton organization. Proteomics 7: 910–920.

Kanelakis KC, Murphy PJ, Galigniana MD, Morishima Y, Takayama S, Reed JC *et al*. (2000). hsp70 interacting protein Hip does not affect glucocorticoid receptor folding by the hsp90-based chaperone machinery except to oppose the effect of BAG-1. Biochemistry 39: 14314–14321.

Kapturczak MH, Meier-Kriesche HU, Kaplan B (2004). Pharmacology of calcineurin antagonists. Transplant Proc 36 (2 Suppl.): 25S–32S.

Kino T, Hatanaka H, Hashimoto M, Nishiyama M, Goto T, Okuhara M *et al*. (1987). FK-506, a novel immunosuppressant isolated from a Streptomyces. I. Fermentation, isolation, and physico-chemical and biological characteristics. J Antibiot (Tokyo) 40: 1249–1255.

Liu J, Albers MW, Wandless TJ, Luan S, Alberg DG, Belshaw PJ *et al*. (1992). Inhibition of T cell signaling by immunophilin-ligand complexes correlates with loss of calcineurin phosphatase activity. Biochemistry 31: 3896–3901.

McCarthy KD, de Vellis J (1980). Preparation of separate astroglial and oligodendroglial cell cultures from rat cerebral tissue. J Cell Biol 85: 890–902.

Murphy PJ, Morishima Y, Chen H, Galigniana MD, Mansfield JF, Simons SS *et al*. (2003). Visualization and mechanism of assembly of a glucocorticoid receptor. Hsp70 complex that is primed for subsequent Hsp90-dependent opening of the steroid binding cleft. J Biol Chem 278: 34764–34773.

Picard D (2006). Intracellular dynamics of the Hsp90 co-chaperone p23 is dictated by Hsp90. Exp Cell Res 312: 198–204.

Pratt WB, Galigniana MD, Harrell JM, DeFranco DB (2004). Role of hsp90 and the hsp90-binding immunophilins in signalling protein movement. Cell Signal 16: 857–872.

Price RD, Yamaji T, Matsuoka N (2003). FK506 potentiates NGF-induced neurite outgrowth via the Ras/Raf/MAP kinase pathway. Br J Pharmacol 140: 825–829.

Quintá HR, Maschi D, Gomez-Sanchez C, Piwien Pilipuk G, Galigniana MD (2010). Subcellular rearrangement of hsp90-binding immunophilins accompanies neuronal differentiation and neurite outgrowth. J Neurochem 115: 716–734.

Sivils JC, Storer CL, Galigniana MD, Cox MB (2011). Regulation of steroid hormone receptor function by the 52-kDa FK506-binding protein (FKBP52). Curr Opin Pharmacol 11: 314–319.

Terranova R, Pereira CF, Du Roure C, Merkenschlager M, Fisher AG (2006). Acquisition and extinction of gene expression programs are separable events in heterokaryon reprogramming. J Cell Sci 119 (Pt 10): 2065–2072.

Trivedi N, Jung P, Brown A (2007). Neurofilaments switch between distinct mobile and stationary states during their transport along axons. J Neurosci 27: 507–516.

Vicari-Christensen M, Repper S, Basile S, Young D (2009). Tacrolimus: review of pharmacokinetics, pharmacodynamics, and pharmacogenetics to facilitate practitioners' understanding and offer strategies for educating patients and promoting adherence. Prog Transplant 19: 277–284.

Wallemacq P, Armstrong VW, Brunet M, Haufroid V, Holt DW, Johnston A *et al*. (2009). Opportunities to optimize tacrolimus therapy in solid organ transplantation: report of the European consensus conference. Ther Drug Monit 31: 139–152.

Wang X, Pongrac JL, DeFranco DB (2002). Glucocorticoid receptors in hippocampal neurons that do not engage proteasomes escape from hormone-dependent down-regulation but maintain transactivation activity. Mol Endocrinol 16: 1987–1998.